Paper No. 907. (quote when citing this article)
Eleventh World Conference on Earthquake Engineering
ISBN: 0 08 042822 3

REFLECTIVITY STRUCTURE BENEATH SAN FERNANDO VALLEY, CALIFORNIA, USING SEISMICITY DATA AND EXPLORATION SEISMOLOGY TECHNIQUES

SERGIO CHÁVEZ-PÉREZ and JOHN N. LOUIE

Seismological Laboratory/174, Mackay School of Mines,
University of Nevada, Reno,
Reno, NV 89557-0141, USA.
Internet: sergio@seismo.unr.edu

ABSTRACT

Earthquake hazard assessment in the San Fernando Valley, California, requires knowledge of the existence and geometry of blind thrust faults. Crustal-scale reflection imaging for this region is feasible using seismicity data from a regional network of short period vertical seismometers. Regional fault structures are imaged from the reflectivity structure beneath the aftershock zone of the 1994 Northridge earthquake. Work presented here combines simple data editing and summation techniques borrowed from exploration seismology. Results show the potential of migrated depth sections in defining major reflectors and suggest that the use of existing aftershock data offers an economic and straightforward alternative for an integration of seismic reflection data in the area.

KEYWORDS

Reflectivity; seismic imaging; depth migration; Kirchhoff migration; exploration seismology; seismicity data; short period data; aftershock data; Northridge earthquake; San Fernando Valley; California.

INTRODUCTION

The broad destruction caused by the 17 January 1994 Northridge earthquake on a thrust fault buried in the heavily-urbanized San Fernando Valley, California, emphasizes the need for better understanding of the structure and potential hazard of blind thrust fault systems.

Acoustic imaging using exploration seismology tools and earthquake sources allows us to produce reflection views of the crust to depths where other data are commonly not available. For instance, James *et al.* (1987) obtained near-vertical reflection profiles in regions of shallow seismicity, and Spudich and Bostwick (1987) capitalized on the principle of seismic reciprocity to form apparent receiver arrays from event clusters, allowing them to derive apparent velocity information from a few stations recording many events.

Morales and McMechan (1990) illustrated earthquake source imaging based on finite-difference extrapolation, and reviewed the acoustic and elastic cases. They found that, in principle, earthquake recordings allow for reconstruction of the source properties, locations and fault orientations. Also, Rietbrock and

Scherbaum (1994) describe numerical examples and a successful case of a well-focused acoustic image of one earthquake source.

Analyses of scattered waves using stacking and Kirchhoff migration have also proven useful in the evaluation of generalized site effects and earthquake hazard (Spudich and Miller, 1990; Spudich and Iida, 1993; Revenaugh, 1995a, b, c).

As in oil industry seismic-reflection surveying, imaging of structure through high-frequency reflectivity demands high-multiplicity data, or a large number of overlapping sources and receivers. Despite the intrinsic limitations of close source spacing (because of multiple events) and wide station spacing, initial work (Chávez-Pérez and Louie, 1995) showed that a small cluster of tens of aftershocks has the spatial sampling needed to image crustal reflectors beneath the Northridge aftershock zone. In addition, the close spatial distribution of Northridge aftershocks illuminates (Fig. 1) structures not previously mapped at depth (Hauksson *et al.*, 1995). In this case a reliable velocity structure over the three-dimensional (3-d) array of sources (aftershocks) and receivers (network stations) provides the information needed to locate crustal reflectors in cross sections or 3-d volumes.

The main purpose of this work is to image the structure beneath San Fernando Valley using Northridge aftershocks and a combination of simple data editing and Kirchhoff depth migration.

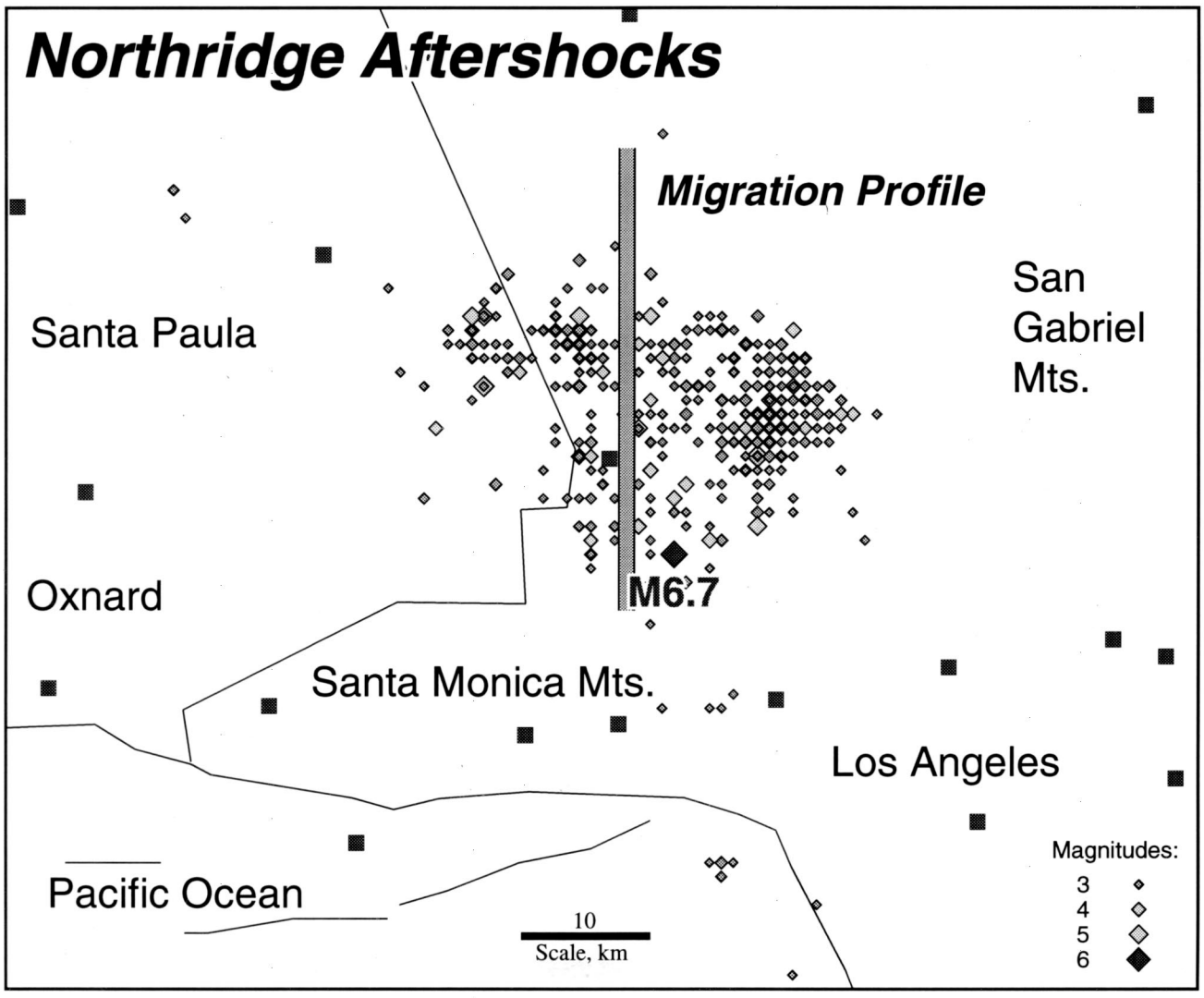

Fig. 1. Map locating the 1994 Northridge, California, main shock (M6.7), aftershocks (closed diamonds, M≥3), the migration profile (south-north line) and some receivers (closed squares).

DATA SELECTION AND PREPROCESSING

Data are short period vertical component seismograms from the Southern California Seismic Network (SCSN) provided through the Southern California Earthquake Center (SCEC) Data Center.

Earthquake locations of the SCEC Data Center are used in this work and 3-d velocity models and relocations will be used in future work. For the time being, well-located, A-quality aftershocks (magnitude ≥ 3) lying within 3 km depth are used in the analyses.

To project a reflected wave in a seismogram to a reflector location one needs to know the time of the arrival, and be able to characterize it as having significant amplitude within the seismogram. Stacking and migration find events that have some coherency across a source-receiver array (of events in this case) and sum amplitudes to reject uncorrelated noise. Coherent reflections can thus be obtained, for instance, by common midpoint stacking (Chávez-Pérez and Louie, 1995) to improve the signal-to-noise ratio or even by simple vertical stacking (Fig. 2).

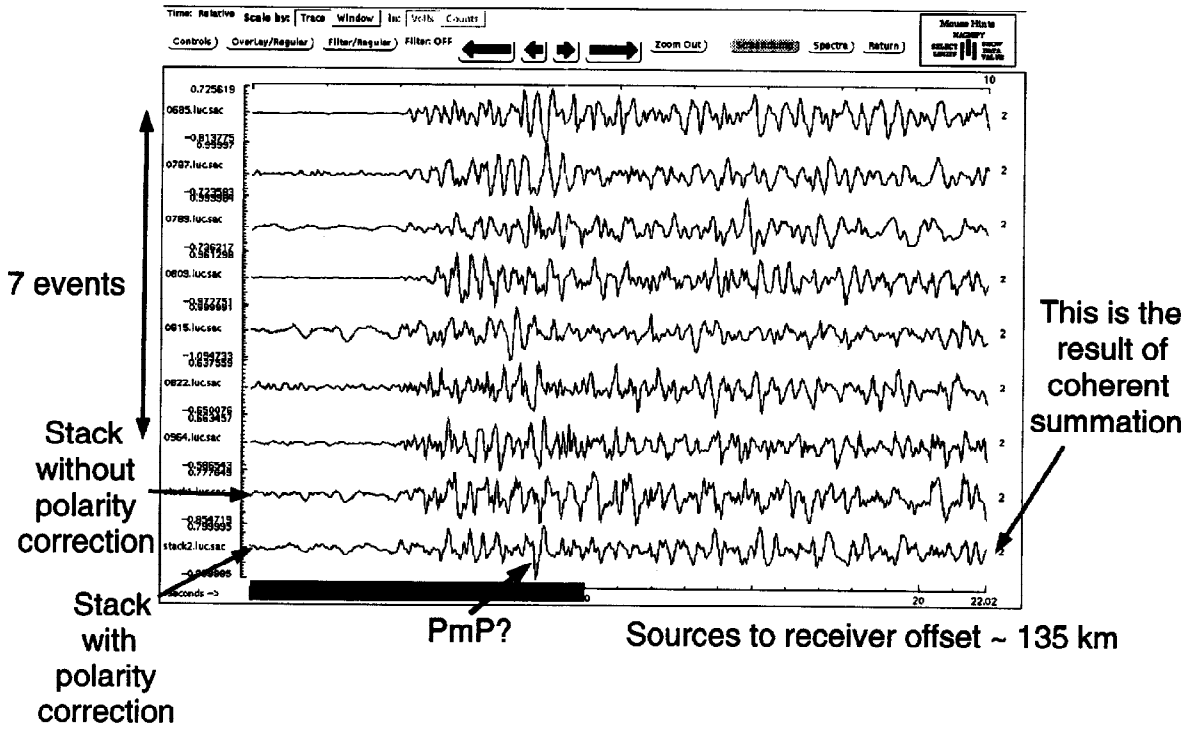

Fig. 2. Example of coherent summation. Common receiver gather of seven events recorded at the Lucerne (LUC) station. P_mP depicts a possible reflection from the Moho.

For the sake of attaining coherent summations, only data with high-quality impulsive P wave picks are used to correct for sign reversals due to varying focal mechanisms.

Clipped and saturated records are quite common in short-period data and are regarded as sign-bit recordings (O'Brien *et al.*, 1982). With sufficient data redundancy, stacking and migration are often able to recover geometric information. Record sections include 200 km in epicentral distance and 30 s

duration to include wide-angle reflections between first compressional, P_g, and first shear, S_g, arrivals. Muting outside the window between P_g and S_g traveltime branches is applied to extract only compressional arrivals, mostly P_g, P_mP and S-P converted energy.

The effects of varying focal mechanisms, absolute wavelet phase, and absolute amplitude variations are encompassed by processing without addressing them directly. Preprocessing includes bandpass filtering (1-40 Hz) and trace equalization for intersource amplitude balancing (*i.e.*, the amplitudes are normalized so that the mean-squared amplitude over the whole trace is the same for all traces). This is equivalent to energy normalization for varying magnitudes.

DEPTH SECTIONS

Based on subsurface projection of surface geology and integration of deep oil-well data, Davis and Namson (1994) proposed a balanced cross-section of the 1994 Northridge earthquake. They interpreted the Santa Susana Mountains and Santa Monica mountains anticlinoria as crustal-scale fault-propagation folds above the Pico and Elysian Park thrusts, respectively. If this is the case, expected reflections would be coming from the main thrust faults and a mid-crustal detachment where the Elysian Park thrust supposedly roots at 22 km depth (Davis and Namson, 1994).

Picking fault locations and interpreting the core of a fault-propagation fold are problematic because of large lateral velocity changes. Synthetic examples show that most of the reflected events arise from the basal detachment and depth migration is required to obtain a reasonable subsurface image (Morse *et al.*, 1991).

Kirchhoff depth migration produces an image of subsurface reflectors. One fundamental assumption used in this process is that the primary reflected energy, when treated as a P-P scattering problem, is isotropic (Wu and Aki, 1985). The image is obtained by summing the data at traveltimes computed through a background velocity model.

The Kirchhoff depth migration process used is similar to that utilized by Louie *et al.* (1988). The migration is a back projection of assumed primary reflection amplitudes into a depth section. It has been identified by Le Bras and Clayton (1988) as the tomographic inverse of the acoustic wave equation under the Born approximation in the far field, utilizing WKBJ rays for downward continuation and two-way reflection travel time for the imaging condition. Travel times are computed with Vidale's (1988) finite-difference solution to the eikonal equation.

Depth sections depict reflectivity along a 50 km south-north migration profile (Fig. 1) by using 3-d Kirchhoff depth migration with Hadley and Kanamori's (1977) one-dimensional (1-d) P wave velocity model shown in Table 1.

Table 1. Hadley and Kanamori's (1977) flat-layer velocity model for southern California.

Velocity km/s	Depth km
5.5	0.0
6.3	5.5
6.7	16.0
7.8	32.0

Figure 3 shows that the final depth imaging result is obtained by stacking the migrated partial images for each event (Fig. 3). Note here that data in each record section is defined only by a window of compressional arrivals (denoted by gray).

One of the major problems in Kirchhoff depth migration is image resolution. When the method is applied to data with limited observation geometry, artifacts or false images appear and make the results difficult to interpret. In this case sparse receiver coverage causes artifacts along elliptical trajectories in the migrated depth section. Unfocusing of *P-S* and *S-P* converted energy also contributes to image degradation.

Figure 4a shows a crustal reflectivity depth section of data from 27 A-quality aftershocks (823 seismograms) lying within 3 km depth. Datum is at sea level. Black shows positive reflectivity, white shows negative reflectivity and gray shows no reflectivity. This section provides estimates of image resolution, migration artifacts and ray coverage for the region of interest.

Artifacts due to poor reflection coverage show kinks in the nearly vertical trajectories they define. These are due to propagation through the 1-d velocity model and are clearly seen at the deepest interface, the Moho, at about 32 km depth.

Strong dipping reflectors appear that do not follow the trajectories defined by the artifacts. They seem to correlate closely with the position of the Pico and Elysian Park thrusts, but extend below the projected depth of the proposed mid-crustal detachment. Note that there is a dipping reflector almost parallel to the Elysian Park thrust. One can also distinguish some nearly horizontal reflectors at depths between 20-25 km. However, they do not depict clear evidence for a mid-crustal detachment. It is hoped that structural definition will improve after summing many more record sections and using 3-d velocity models (Mori *et al.*, 1995; Zhao and Kanamori, 1995; Pujol, 1996).

Figure 4b shows the depth section of Fig. 4a with Northridge main shock, A-quality aftershocks (magnitude $\geq$3) at all depths, and the thrust faults and mid-crustal detachment, proposed by Davis and Namson (1994), superimposed. Note how the Pico and Elysian Park thrusts correlate with some of the main dipping reflectors.

Future work will focus on improving structural definition and detail, determining, through statistical analysis, what migrated structures are real and which are artifacts due to noisy data and poor reflection coverage, and correcting for varying radiation patterns for those events with known focal mechanisms.

CONCLUSIONS

Data processing of a few events permits the identification of major reflectors near the main blind thrust faults proposed by earthquake geologists beneath San Fernando Valley and perhaps some deeper structures.

ACKNOWLEDGMENTS

This work was funded by a US National Science Foundation grant (EAR-9416224). The first author acknowledges financial support by CONACYT, Mexico's National Council for Science and Technology. Aftershock data were recorded by the Southern California Seismic Network (SCSN) which is operated jointly by the Seismological Laboratory at Caltech and the US Geological Survey, Pasadena, CA. Steven Jaumé obtained the data set used here and helped to prepare Fig. 2. Glenn Biasi and Serdar Özalaybey read the manuscript and helped to improve its clarity.

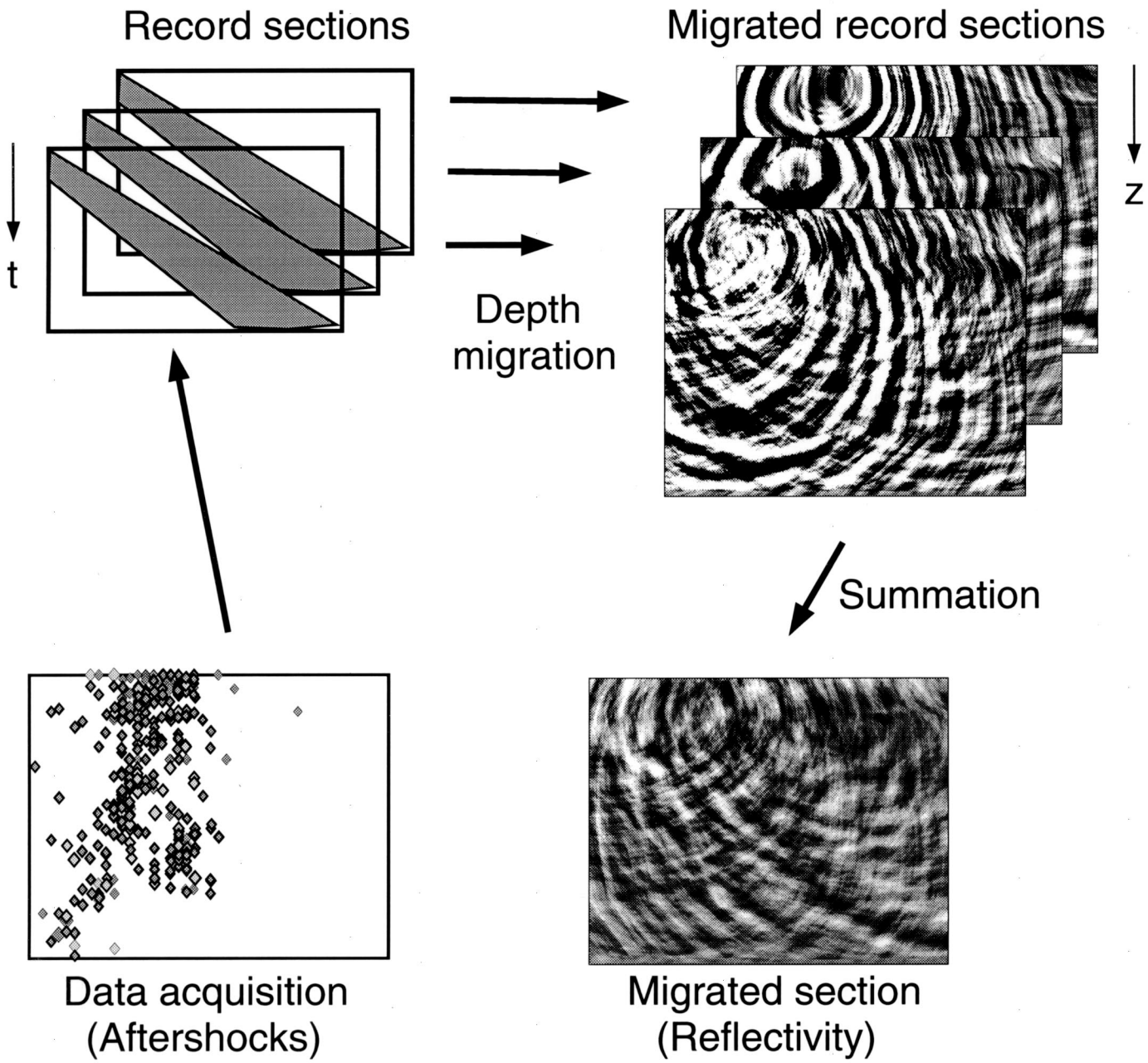

Fig. 3. Migration of record sections. Each record is migrated individually along the migration profile shown in Fig. 1. The depth migrated results are summed to obtain the crustal reflectivity section.

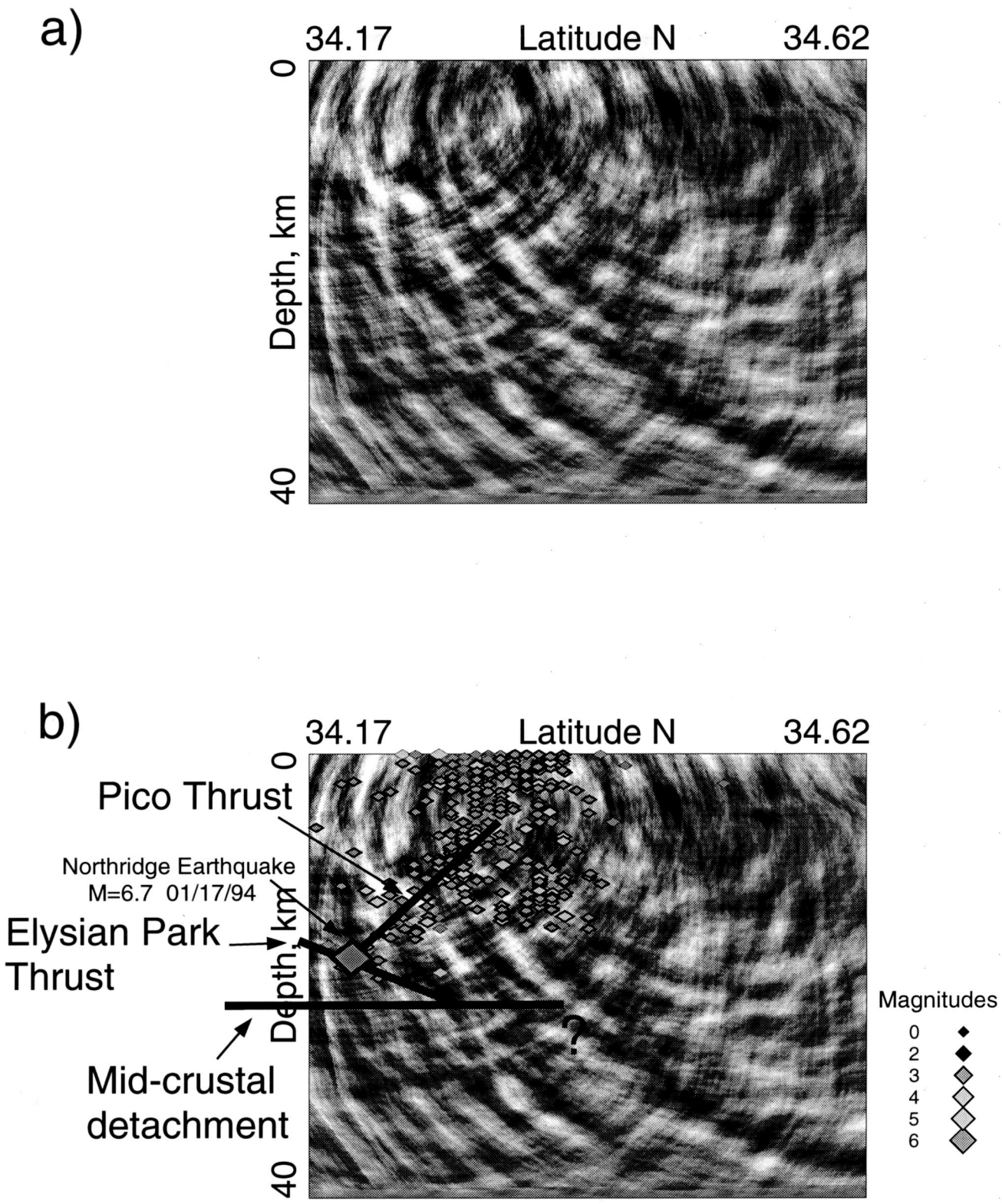

Fig. 4. a) Crustal reflectivity depth section along the migration profile (Fig. 1). b) Same image as in (a) with Northridge main shock, aftershocks and the interpretation of Davis and Namson (1994) superimposed.

REFERENCES

Chávez-Pérez, S. and J.N. Louie (1995). Seismic reflection views of a blind thrust fault system using earthquake data. *65th Annual Int. Mtg., Society of Exploration Geophysicists, Expanded Abstracts*, 511-514, Houston, TX, October 8-13.

Davis, T.L. and J.S. Namson (1994). A balanced cross-section of the 1994 Northridge earthquake, southern California. *Nature*, **372**, 167-169.

Hadley, D. and H. Kanamori (1977). Seismic structure of the Transverse Ranges, California. *Geol. Soc. Am. Bull.*, **88**, 1469-1478.

Hauksson, E., L.M. Jones, and K. Hutton (1995). The 1994 Northridge earthquake sequence in California: Seismological and tectonic aspects. *J. Geophys. Res.*, **100**, 12335-12355.

James, D.E., T.J. Clarke, and R.P. Meyer (1987). A study of seismic reflection imaging using microearthquake sources. *Tectonophysics*, **140**, 65-79.

Le Bras, R.J. and R.W. Clayton (1988). An iterative inversion of backscattered acoustic waves. *Geophysics*, **53**, 501-508.

Louie, J.N., R.W. Clayton, and R.J. Le Bras (1988). 3-d imaging of steeply dipping structure near the San Andreas fault, Parkfield, California. *Geophysics*, **53**, 176-185.

Morales, J. and G.A. McMechan (1990). Imaging of earthquake sources. *Int. J. of Imaging Systems and Technology*, **2**, 231-238.

Mori, J., D.J. Wald, and R.L. Wesson (1995). Overlapping fault planes of the 1971 San Fernando and 1994 Northridge, California earthquakes. *Geophys. Res. Lett.*, **22**, 1033-1036.

Morse, P.F., G.W. Purnell, and D.A. Medwedeff (1991). Seismic modeling of fault-related folds. In: *Seismic Modeling of Geologic Structures, Applications to Exploration Problems* (S.W. Fagin, ed.), pp. 127-152. Society of Exploration Geophysicists, Tulsa, OK.

O'Brien, J.T., W.P. Kamp, and G.M. Hoover (1982). Sign-bit amplitude recovery with applications to seismic data. *Geophysics*, **47**, 1527-1539.

Pujol, J. (1996). An integrated 3D-velocity inversion – JHD relocation analysis of events in the Northridge area. *Bull. Seism. Soc. Am.*, **86**, in press.

Revenaugh, J. (1995a). The contribution of topographic scattering to teleseismic coda. *Geophys. Res. Lett.*, **22**, 543-546.

Revenaugh, J. (1995b). A scattered-wave image of subduction beneath the Transverse Ranges, California. *Science*, **268**, 1888-1892.

Revenaugh, J. (1995c). Relation of the 1992 Landers, California, earthquake sequence to seismic scattering. *Science*, **270**, 1344-1347.

Rietbrock, A. and F. Scherbaum (1994). Acoustic imaging of earthquake sources from the Chalfant Valley, 1986, aftershock series. *Geophys. J. Int.*, **119**, 260-268.

Spudich, P. and T. Bostwick (1987). Studies of the seismic coda using an earthquake cluster as a deeply buried seismograph array. *J. Geophys. Res.*, **92**, 10526-10546.

Spudich, P. and M. Iida (1993). The seismic coda, site effects, and scattering in alluvial basins studied using aftershocks of the 1986 North Palm Springs, California, earthquake as source arrays. *Bull. Seism. Soc. Am.*, **83**, 1721-1743.

Spudich, P. and D.P. Miller (1990). Seismic site effects and the spatial interpolation of earthquake seismograms: Results using aftershocks of the 1986 North Palm Springs, California, earthquake. *Bull. Seism. Soc. Am.*, **80**, 1504-1532.

Vidale, J.E. (1988). Finite-difference calculation of travel times. *Bull. Seism. Soc. Am.*, **78**, 2062-2076.

Wu, R. and K. Aki (1985). Scattering characteristics of elastic waves by an elastic heterogeneity. *Geophysics*, **50**, 582-595.

Zhao, D. and H. Kanamori (1995). The 1994 Northridge earthquake: 3-D crustal structure in the rupture zone and its relation to the aftershock locations and mechanisms. *Geophys. Res. Lett.*, **22**, 763-766.